

# Non-linear evolution of thermally unstable slim accretion discs with a diffusive form of viscosity

Ewa Szuszkiewicz<sup>1,2,3,4</sup> and John C. Miller<sup>4,5</sup>

<sup>1</sup> Institute of Physics, University of Szczecin, ul. Wielkopolska 15, 70-451 Szczecin, Poland

<sup>2</sup> Toruń Centre for Astronomy, Nicolaus Copernicus University, ul. Gagarina 11, 87-100 Toruń, Poland

<sup>3</sup> Dipartimento di Fisica “Galileo Galilei”, Università degli Studi di Padova, via Marzolo 8, 35131 Padova, Italy

<sup>4</sup> International School for Advanced Studies, SISSA, via Beirut 2-4, 34014 Trieste, Italy

<sup>5</sup> Nuclear and Astrophysics Laboratory, University of Oxford, Keble Road, Oxford OX1 3RH, England

Accepted . Received ; in original form

## ABSTRACT

We are carrying out a programme of non-linear time-dependent numerical calculations to study the evolution of the thermal instability driven by radiation pressure in transonic accretion discs around black holes. In our previous studies we first investigated the original version of the slim-disc model with low viscosity ( $\alpha = 0.001$ ) for a stellar-mass ( $10M_\odot$ ) black hole, comparing the behaviour seen with results from local stability analysis (which were broadly confirmed). In some of the unstable models, we saw a violently evolving shock-like feature appearing near to the sonic point. Next, we retained the original model simplifications but considered a higher value of  $\alpha$  ( $= 0.1$ ) and demonstrated the existence of limit-cycle behaviour under suitable circumstances. The present paper describes more elaborate calculations with a more physical viscosity prescription and including a vertically integrated treatment of acceleration in the vertical direction. Limit-cycle behaviour is still found for a model with  $\alpha = 0.1$ , giving a strong motivation to look for its presence in observational data.

**Key words:** accretion, accretion discs - instabilities

## 1 INTRODUCTION

The aim of the research programme, of which the present paper forms a part, is to study the origin of the incipient instabilities operating in accretion discs around black holes and to investigate their observational consequences for diverse astronomical phenomena. For doing this, we use a class of simple vertically-integrated, non-self-gravitating models of transonic accretion discs. This is well justified because, despite the ongoing development of increasingly sophisticated large-scale numerical models, simple disc modelling still remains the central link between theory and observations. Some of the results of disc phenomenology might be truly fundamental, while others might have more limited domains of applicability (Balbus & Papaloizou, 1999). It would be particularly valuable to determine the sensitivity of the disc solutions to the form of the viscous stress and here we study how the global evolution of the thermal instability driven by radiation pressure depends on the viscosity prescription. This investigation follows on naturally from the overall strategy of our research programme. The model treated in our previous papers (Szuszkiewicz & Miller 1997, 1998 - hereafter Papers I and II) did not yet include several important non-local effects, and in particular, it did not contain a diffusion-type formulation for the viscosity. Those results represent a suitable standard reference for making

comparison with the results from our present calculations in which a diffusion-type formulation for viscosity replaces the  $\alpha$  prescription used previously.

The  $\varphi r$  component of the viscous stress tensor, which is responsible for the transport of angular momentum in a disc, is normally written in the standard form

$$\tau_{\varphi r} = \rho \nu r \frac{\partial \Omega}{\partial r}, \quad (1)$$

where  $\rho$  is the density,  $\nu$  is a kinematic viscosity coefficient and  $\Omega$  is the angular velocity of matter in the disc. However, the relevant viscosity mechanism for accretion discs is clearly not molecular viscosity (which is much too small to be of interest in these circumstances) but instead is some sort of magnetic or turbulent viscosity. For a general turbulent viscosity,

$$\nu_{turb} \sim v_{turb} \ell_{turb}, \quad (2)$$

where  $v_{turb}$  and  $\ell_{turb}$  are the characteristic circulation velocity and length-scale for the turbulent cells (see Kato, Fukue & Mineshige 1998), and then it is common to write

$$\nu = \alpha H c_s, \quad (3)$$

where  $c_s$  is the local sound speed,  $H$  is the half-thickness of

the disc and

$$\alpha \sim \left( \frac{v_{turb}}{c_s} \right) \left( \frac{\ell_{turb}}{H} \right) \quad (4)$$

is a quantity which must be less than or comparable to unity if the turbulence is subsonic with the turbulent cells being confined within the disc. This treatment arises from discussions of viscosity associated with hydrodynamic turbulence (von Weizsäcker 1948) but a similar formula can be appropriate for magnetic viscosity in some circumstances (Shakura & Sunyaev 1973; see also Hawley, Balbus & Stone 2001).

The form of the viscosity plays a key role for the way in which the disc responds to thermal fluctuations. An infinitesimal perturbation giving a small rise in temperature would cause the disc to swell up and, according to Eq. (3), would have the tendency to make it more viscous giving increased heating (although this also depends on how  $\alpha$  changes in response to the perturbation). At the same time, the cooling rate will also become higher as a result of the higher temperature. If the increase of cooling is greater than the increase in heating, the situation is stable with the configuration returning back towards its initial state; however, if the increase of heating is greater than the increase in cooling, the situation is *thermally unstable* with the temperature continuing to increase away from the initial value until the effect is eventually saturated in a non-linear regime. Whether this kind of thermal instability can occur in practice for real discs depends on how fast the viscosity increases as the temperature is increased and this is something which is still under debate. Our view is that it is certainly of interest to study the possible consequences of this thermal instability if it were to arise and then to see whether evidence for it is revealed by observations. This is the line being taken for the present programme of work and, for simplicity, we follow the precedent of using the viscosity formula (3) with constant  $\alpha$  (which does allow for the instability to occur if the accretion rate is high enough).

Within the framework of the above discussion, there is a further simplification which is frequently made. If one considers a stationary Newtonian Keplerian disc and makes a number of approximations (including assuming vertical hydrostatic equilibrium and integrating analytically in the vertical direction), it can be shown that expressions (1) and (3) lead to

$$\tau_{\varphi r} = -\alpha p, \quad (5)$$

where  $p$  is the pressure and  $\alpha$  has been rescaled so as to remove a numerical constant from the formula. This is the well-known  $\alpha p$  prescription of Shakura & Sunyaev (1973) which has been widely used as a general approximate form for the viscous stress even under conditions different from those for which the formula was derived.

Abramowicz et al. (1988), calculated a sequence of vertically-integrated *slim* accretion disc models, using the  $\alpha p$  viscosity prescription but dropping the Keplerian flow condition and including the effects of relativistic gravity in an approximate way by using the pseudo-Newtonian potential of Paczyński & Wiita (1980). Doing this, they found that if  $\dot{M}$  (the accretion rate) is plotted against the surface density  $\Sigma$  for a fixed location in the disc, an S-shaped curve is obtained. This suggested the possibility of having a

limit-cycle behaviour associated with a thermal instability driven by radiation pressure. The results of non-linear time-dependent calculations performed by Honma, Matsumoto & Kato (1991) strongly indicated that such a limit-cycle could indeed occur and the first complete solution of this type was then subsequently obtained by Szuszkiewicz & Miller (1998). This finding, if confirmed by less approximate calculations, would have important consequences for the interpretation of observations. A first step towards checking its robustness is to replace the  $\alpha p$  prescription by the one given directly by Eq. (1) together with expression (3) for  $\nu$ . Doing this makes an important change in the mathematical nature of the system of equations, introducing a parabolic diffusion-type term into an otherwise hyperbolic system.

Until now, little work has been directed towards studying transonic accretion discs with this more general viscosity prescription because the direct integration of the equations is extremely difficult (Hoshi and Shibasaki 1977, Shibasaki 1978). The numerical results of Chen & Taam, (1993), who examined steady state accretion discs, demonstrated that the S-shaped form of the  $\dot{M}(\Sigma)$  curve is insensitive to the form used for the viscous stress. Papaloizou & Szuszkiewicz (1994b) constructed models for the inner part of a transonic adiabatic accretion disc, assuming constant specific angular momentum and including a full treatment of the vertical structure, and for comparison purposes constructed the corresponding one-dimensional viscous-disc models derived under vertical-averaging assumptions (see also Papaloizou & Szuszkiewicz, 1994a). They also investigated causality considerations connected with the formulation of viscosity as a diffusion process and concluded that if the specific angular momentum gradient is very small when the radial velocities are significant, the corrections due to finite propagation effects become small so that the Shakura & Sunyaev (1973) treatment should be reasonably good. Constraints arising from causality considerations may be important though as far as the uniqueness of the steady-state flow is concerned. Both  $\alpha p$  and diffusive viscosity prescriptions have been investigated by Artemova, Bisnovatyi-Kogan, Igumenshchev and Novikov (2000). They found that the stationary solutions for the two types of prescription are very similar for  $\alpha \leq 0.1$  but begin to differ at larger  $\alpha$ . They also showed that the solutions with the diffusive shear stress have one singular point which is always of the saddle type. A similar result had been obtained by Papaloizou & Szuszkiewicz (1994a) for transonic accretion discs with a polytropic equation of state. The aim of our present study is to investigate the effect of using a diffusive form of viscosity in global non-linear time-dependent calculations of thermally unstable slim-disc models.

The plan of the paper is as follows. In Section 2, we discuss the set of basic equations used for our present calculations, highlighting the changes with respect to the equations used in Papers I and II. The modifications in the numerical treatment are described in Section 3. In Section 4 we present the new results obtained with the revised computer code and compare them with those obtained previously with the  $\alpha p$  prescription. Section 5 contains comments and conclusions.

## 2 WHAT IS NEW IN THE SET OF EQUATIONS?

The basic equations used for describing the evolution of the thermal instability in an axisymmetric, non-self-gravitating, optically-thick disc were presented in full detail in Paper I and the treatment which we will be using for parts of the flow which are not optically thick was described in Paper II. The assumptions and strategy used for the calculations have been fully described in these earlier papers. Here we point out and discuss two new features which we are now introducing into the set of equations: the direct use of formula (1) for the viscous stress (giving dependence on  $\partial\Omega/\partial r$ ) and the introduction of a new dynamical equation for the vertical acceleration (abandoning the previous approximation of taking hydrostatic equilibrium to hold in the vertical direction).

In cylindrical polar coordinates  $(r, \varphi, z)$  centred on the black hole (having mass  $M$ ), our basic hydrodynamical equations are as follows. The conservation of mass equation

$$\frac{D\Sigma}{Dt} = -\frac{\Sigma}{r} \frac{\partial}{\partial r} (rv_r) \quad (6)$$

and the conservation of radial momentum

$$\frac{Dv_r}{Dt} = -\frac{1}{\rho} \frac{\partial p}{\partial r} + \frac{(l^2 - l_K^2)}{r^3} \quad (7)$$

are the same as in Papers I and II. We are using the following notation:  $D/Dt$  is the Lagrangian derivative given by

$$\frac{D}{Dt} = \frac{\partial}{\partial t} + v_r \frac{\partial}{\partial r}, \quad (8)$$

$\Sigma = \Sigma(r, t)$  is the surface density obtained by vertically integrating the mass density  $\rho$ ,  $v_r = Dr/Dt$ ,  $p$  is the total pressure,  $l = l(r, t) = rv_\varphi(r, t)$  is the specific angular momentum,  $l_K$  is the value of  $l$  for Keplerian motion in the pseudo-Newtonian potential with  $v_\varphi = [GMr/(r - r_G)^2]^{1/2}$ , where  $r_G$  is the Schwarzschild radius of the black hole, and  $\Omega_K = v_\varphi/r$ . Note that  $v_r$  is negative for an inflow and that the  $\rho$  and  $p$  appearing in Eq. (7) refer to values in the equatorial plane.

The form of the azimuthal equation of motion used in the previous calculations

$$\frac{Dl}{Dt} = -\frac{\alpha}{r\Sigma} \frac{\partial}{\partial r} (r^2 p H) \quad (9)$$

was obtained from

$$\frac{Dl}{Dt} = \frac{1}{r\Sigma} \frac{\partial}{\partial r} \left( r^2 2 \int_0^H \tau_{\varphi r} dz \right) \quad (10)$$

using the  $\alpha p$  viscosity prescription given by Eq. (5). Here, instead, we use the expression given directly by Eqs. (1) and (3):

$$\tau_{\varphi r} = \rho \alpha c_s H r \frac{\partial \Omega}{\partial r}, \quad (11)$$

and Eq. (10) then gives

$$\frac{Dl}{Dt} = \frac{\alpha}{r\Sigma} \frac{\partial}{\partial r} \left( r^3 c_s H \Sigma \frac{\partial \Omega}{\partial r} \right). \quad (12)$$

Note that, as mentioned earlier, the  $\alpha$  appearing here is rescaled with respect to that used previously with the  $\alpha p$  prescription. The value of the rescaling factor depends on the way in which the vertical structure is treated. In Paper

I, we described in detail how this was done in our previous work and next we will give a modified discussion of how it is done in the calculations of the present paper.

The vertical equation of motion can be written in the form

$$\frac{Dv_z}{Dt} = -\frac{1}{\rho} \frac{\partial p}{\partial z} - \frac{\partial \Phi}{\partial z} + F_{zz}, \quad (13)$$

where  $\Phi$  is the pseudo-Newtonian potential given by  $\Phi = -GM/(R - r_G)$ , with  $R^2 = r^2 + z^2$ , and  $F_{zz}$  is a viscous force which is set to zero throughout the present work. The strategy of the slim disc approach is to proceed by deriving a vertically-integrated form of this equation, making use of the fact that the disc is taken to be thin enough so that the gravitational potential  $\Phi$  can be expanded in the vertical direction in powers of  $z/r$  and only the lowest-order terms retained. We then need two further assumptions about variations of quantities in the vertical direction in order to be able to make the integration. The pressure and density,  $p$  and  $\rho$ , are taken to be linked together (in the vertical direction) by a polytropic relation  $p \propto \rho^{1+1/N}$ , where  $N$  is the polytropic index. Additionally, we need to assume something about the vertical velocity and in the previous work (in common with the preceding literature on slim discs) this condition was provided by assuming vertical hydrostatic equilibrium to hold so that  $Dv_z/Dt = 0$ . The equation could then be vertically integrated to give (after some manipulation and setting  $N = 2$  following Paczyński & Bisnovatyi-Kogan 1981):

$$\Omega_K^2 H^2 = 6 \frac{p}{\rho}. \quad (14)$$

This formula applies for strictly Newtonian gravity as well as with the pseudo-Newtonian potential which we are using here. Inserting expression (14) into the Newtonian argument leading to the  $\alpha p$  formula, one obtains that  $\alpha_2$  (the  $\alpha$  in the  $\alpha p$  formula) is related to the original  $\alpha$ , as in equation (1), by

$$\alpha_2 = \frac{3\sqrt{6}}{2} \alpha_1 \quad (15)$$

We will use this relationship for calculating models within the new approach which are “equivalent” to ones with a particular  $\alpha$  in the old formulation.

In Paper I, we commented that neglecting the vertical acceleration may sometimes be a rather poor approximation in some parts of the disc, as suggested by two-dimensional studies (Papaloizou & Szuszkiewicz 1994b), and that investigating the effects of including vertical acceleration in a consistent way was one of the important issues to be addressed subsequently. Contrary to our original strategy of introducing additional modifications one by one, the acceleration term has been included here together with the more general form for the viscosity. This was done because we found that we could not obtain a numerically stable solution with the revised viscosity law unless we also included the vertical acceleration. We will discuss this further in Section 5.

The simplest way of dealing with the acceleration term is to replace the assumption of hydrostatic equilibrium with that of taking  $z/H$  to be constant along fluid flow lines. We note that while this is not in accordance with the results of two-dimensional hydrodynamic simulations (which reveal

a complex circulating flow structure) it is consistent with the general picture of the slim disc approach and therefore seems appropriate here. Introducing this and then making the vertical integration as before, one obtains

$$\frac{DV_z}{Dt} = 6 \frac{p}{\Sigma} - \frac{GM}{(r - r_G)^2} \left( \frac{H}{r} \right), \quad (16)$$

where  $V_z$  is the vertical component of velocity for a fluid element at the top surface of the disc.

The introduction of the diffusive form of viscosity requires changes also in the energy balance equation

$$\rho T \frac{DS}{Dt} = Q_{vis} + Q_{rad}. \quad (17)$$

Here  $T$  is the temperature,  $S$  is the entropy per unit mass,  $Q_{vis}$  is the rate at which heat is generated by viscous friction, now given by

$$Q_{vis} = \rho \nu \left( r \frac{\partial \Omega}{\partial r} \right)^2, \quad (18)$$

and  $Q_{rad}$  is the rate at which heat is lost or gained by means of radiative energy transfer, here given by

$$Q_{rad} = -\frac{F^-}{H}, \quad (19)$$

with  $F^-$  being the radiative flux per unit area away from the disc in the vertical direction (we are neglecting heat conduction through the disc in the radial direction). The vertically-integrated form of the energy balance equation may be written in the following way

$$\frac{DT}{Dt} = \frac{\alpha H r^2 T (\partial \Omega / \partial r)^2}{\sqrt{p/\rho} 0.67(12 - 10.5\beta)} - \frac{TF^-}{0.67pH(12 - 10.5\beta)} + \frac{(4 - 3\beta)}{(12 - 10.5\beta)} \frac{T}{\rho} \frac{D\rho}{Dt} \quad (20)$$

(Note that there is a typographical error in the equivalent equation of Paper I – there equation (17). On the right hand side there should be a minus sign in front of the first term.)

If the medium is optically thick we use the expression

$$F^- = \frac{16\sigma T^4}{\kappa \rho H}, \quad (21)$$

where  $\sigma$  is the Stefan-Boltzmann constant and  $\kappa$  is the opacity. The opacity is approximated by the Kramers formula for chemical abundances corresponding to those of Population I stars

$$\kappa = 0.34 (1 + 6 \times 10^{24} \rho T^{-3.5}) \text{ g}^{-1} \text{ cm}^2. \quad (22)$$

The thermodynamic quantities in the equatorial plane are taken to obey the equation of state

$$p = k\rho T + p_r \quad (23)$$

where  $p_r$  is the radiation pressure given by  $p_r = \frac{a}{3} T^4$ .

If the medium is not optically thick, we follow the approach of Huré et al. (1994) and write

$$F^- = 6 \frac{4\sigma T^4}{\frac{3\tau_R}{2} + \sqrt{3} + \frac{1}{\tau_P}} \quad (24)$$

where  $\tau_R$  and  $\tau_P$  are the Rosseland and Planck mean optical depths (equal to  $\kappa_R \rho H$  and  $\kappa_P \rho H$ ). The expression for the

radiation pressure corresponding to this  $F^-$  is

$$p_r = \frac{F^-}{12c} \left( \tau_R + \frac{2}{\sqrt{3}} \right) \quad (25)$$

For the Rosseland optical depth, we use the expression

$$\tau_R = 0.34 \Sigma (1 + 6 \times 10^{24} \rho T^{-3.5}), \quad (26)$$

corresponding to the expression for  $\kappa$  given by equation (22), while for the Planck optical depth we use

$$\tau_P = \frac{1}{4\sigma T^4} (q_{br}^-) \quad (27)$$

where  $q_{br}^-$  is the bremsstrahlung cooling rate given by

$$q_{br}^- = 1.24 \times 10^{21} H \rho^2 T^{1/2} \text{ erg cm}^{-2} \text{ s}^{-1} \quad (28)$$

Further discussion of this has been given in Paper II.

Our aim here is to investigate the extent to which the inclusion of the more physical viscosity prescription causes differences in non-stationary behaviour with respect to that of the “standard” models calculated in our previous papers.

### 3 WHAT IS NEW IN THE NUMERICAL PROCEDURES?

The equations presented in the previous section have been solved numerically using a modified version of the Lagrangian hydrodynamics code described in detail in Paper I, with the accreting matter being divided into a succession of comoving radial zones and with the difference scheme following the standard pattern for one-dimensional Lagrangian hydrodynamics. In this section we discuss the modifications which have been necessary in order to make a successful calculation for a model with the new viscosity prescription and including the implementation of the dynamical equation for motion in the vertical direction.

The grid structure was modified from that used previously in order to give better resolution where this was most needed. The gridding was extensively tested to show that it was sufficiently fine to be well within the convergent regime and, by experiment, we hope to have found a near optimal compromise between accuracy and computational expense. The inner edge of the grid was set at  $r \approx 2.5r_G$  (whenever the innermost comoving zone was entirely inside  $2.5r_G$ , it was discarded and the grid was remapped following the procedure described in Paper I, using piecewise cubic interpolation). The outer boundary was set at  $r = 10^4 r_G$ , far enough away so that no perturbation from the inner regions could reach as far as this during the time of the calculation. Conditions there were essentially unchanging over this timescale, making it easy to impose outer boundary conditions. For the model described in detail in this paper, we used a grid of 400 comoving zones organised as follows: for the first 59 zones, each one contained a mass 11 per cent larger than the one interior to it; for the next 60 zones, the increase was 5 per cent; for the rest of the disc, with exception of the last 60 zones, the increase was 2.5 per cent and, finally, the last 60 zones had an increase of 12 per cent. This was found to give satisfactory resolution and accuracy.

The equations are solved for  $\Sigma$ ,  $v_r$ ,  $l$ ,  $V_z$  and  $T$ , as the main dependent variables, with  $r$  and  $H$  being calculated from  $Dr/Dt = v_r$  and  $DH/Dt = V_z$  respectively. In our

previous studies the time-step was adjusted in accordance with the Courant condition and with two additional constraints on the fractional variations of  $\rho$  and  $T$  in any single time-step. Now that we have a parabolic term appearing in Eq. (12), it is necessary to add a further time-step condition in order to maintain numerical stability:

$$\Delta t \leq (\Delta r)^2 / (2\nu), \quad (29)$$

where  $\Delta t$  and  $\Delta r$  are the time-step and space-step respectively. In the energy equation (20), which is solved implicitly for  $T$ , the gradient of the angular velocity appearing in the viscous heating term is no longer substituted by the Keplerian value as before.

When  $r$ ,  $\Sigma$ ,  $T$  and  $H$  are known,  $\rho$  can be found directly from  $\rho = \Sigma/H$  while  $p$  follows from the equation of state (23). Previously, the solution for  $p$ ,  $\rho$  and  $H$  was embedded in the iteration loop for  $T$ . Introducing the dynamical equations for  $V_z$  and  $H$  significantly speeds up the code.

At every time-step, it is necessary to supply boundary conditions for  $v_r$  and  $l$  at both the inner and outer edges of the grid. As before, the boundary conditions at the inner edge are set by noting that  $l$  is essentially unchanging for infalling matter there, so that it can be taken as constant in time for the innermost zone, and that the pressure gradient term is having negligible effect there, so that it can be set to zero when calculating  $v_r$  at the inner edge. As noted above, the outer edge is located at such a large radius that conditions there are essentially unchanging over the timescale of the calculation and so  $v_r$  is kept constant in time there while  $l$  is calculated using the Keplerian condition at that point.

As initial conditions for the evolutionary calculations, we again used a stationary transonic disc model calculated with the  $\alpha p$  viscosity prescription. The data from this were then transferred onto the finite-difference grid used for the evolutionary calculations and the  $\alpha$  was suitably rescaled following Eq. (15) for use in expression (3). The quantities transferred were  $r$ ,  $v_r$ ,  $\Sigma$ ,  $T$  and  $H$ ;  $l$  was then calculated on the grid, using the stationary version of equation (7), and  $V_z$  was calculated from the formula:

$$V_z = v_r \frac{dH}{dr}. \quad (30)$$

While treating the vertical equation of motion (13) by means of the approximate form (16) is a great improvement over assuming hydrostatic equilibrium in the vertical direction, it is still greatly simplified, particularly in that it involves taking  $Dv_z/Dt$  to depend linearly on  $z/H$  (which follows from  $z/H$  being constant along flowlines). This ceases to be reasonable when there are rapid dynamic changes in the vertical direction such as those seen when the inner parts of the disc deflate rapidly in the course of the evolution which we will be describing in the next section. In reaching a new steady state after the deflation, the vertical acceleration must inevitably deviate from  $Dv_z/Dt \propto z/H$ . In order to keep the solution regular in these circumstances, we introduced an artificial viscous term  $Q_z \propto \rho V_z^2$  which augments the pressure in the vertical direction when the vertical compression is very rapid. This, to some extent, mimics the real behaviour which would occur in these circumstances and is probably the best that can be done within a vertically integrated approach although, of course, the real answer is to go

to a full 2D (or 3D) calculation! Related with this problem is another one concerned with treating the stage in the immediate aftermath of the deflation when a sharp density spike appears. The rapid compression in the radial direction leads to a bunching of the Lagrangian zones causing some of them to become so narrow that accuracy is lost. This was combatted by adjusting the regridding routine to avoid having ultra-narrow zones and simultaneously increasing the artificial diffusion applied in the radial direction. The increased value of this artificial diffusion coefficient is needed only for a very short time and, while its effect is in the direction of causing a broadening of the spike, it is not the main cause of the broadening seen which takes place over a much longer time than that for which the diffusion is applied.

As noted in Paper I, the process of transferring the initial data onto the finite-difference grid, together with the action of numerical noise which inevitably enters during the calculation, is sufficient for introducing suitable generalised perturbations in the model to trigger growth of unstable modes which may be present.

#### 4 LIMIT CYCLE BEHAVIOUR

In Paper II we presented a complete limit-cycle solution for a model with black hole mass  $M = 10M_\odot$ , initial accretion rate  $\dot{M} = 0.06\dot{M}_{cr}$  and viscosity parameter  $\alpha = 0.1$ . ( $\dot{M}_{cr}$  is the critical accretion rate corresponding to the Eddington luminosity). Here we investigate an equivalent model using the more physical viscosity prescription given directly by equations (1) and (3) (for which  $\tau_{r\varphi} \propto \partial\Omega/\partial r$ ) and including the effects of vertical acceleration by means of Eq. (16). The initial equilibrium model is identical to that used in Paper II which, according to the local stability criterion, is thermally unstable in a region extending from  $4.5 r_G$  to  $17.5 r_G$ .

The main conclusion from our new calculations is that the overall behaviour is very similar to that seen before (and described in Paper II). In particular, we again see a succession of limit-cycles. We here present some additional results and highlight some particular points of interest. The figures presented here should be viewed in conjunction with those of Paper II.

The evolution of the geometrical profile of the disc is shown in Fig. 1 and Figs. 2–5 show the behaviour of the temperature  $T$ , the surface density  $\Sigma$ , the effective optical depth  $\tau_{eff}$  and the local accretion rate  $\dot{m}$  at times corresponding to the first five panels of Fig. 1. (No curves are drawn corresponding to the sixth panel in order to avoid the figures becoming over-complicated.) In order to check for possible long-term variations, we continued the calculation for a total of twenty complete cycles; the results shown in Fig. 1 are for a representative cycle – the 17th.

The first panel of Fig. 1 shows the disc just before the start of the cycle (which we define to be the moment when the instability first begins to exponentiate). As the instability sets in, the temperature in the unstable region rises rapidly above its stationary value, increasing the contribution of the radiation pressure by nearly an order of magnitude. The heated material expands in all directions, pushing inner material into the black hole, expanding the disc vertically and launching a compression wave out through the disc which sweeps matter ahead of it leaving a semi-evacuated region behind. This is the stage reached by 2 seconds into the

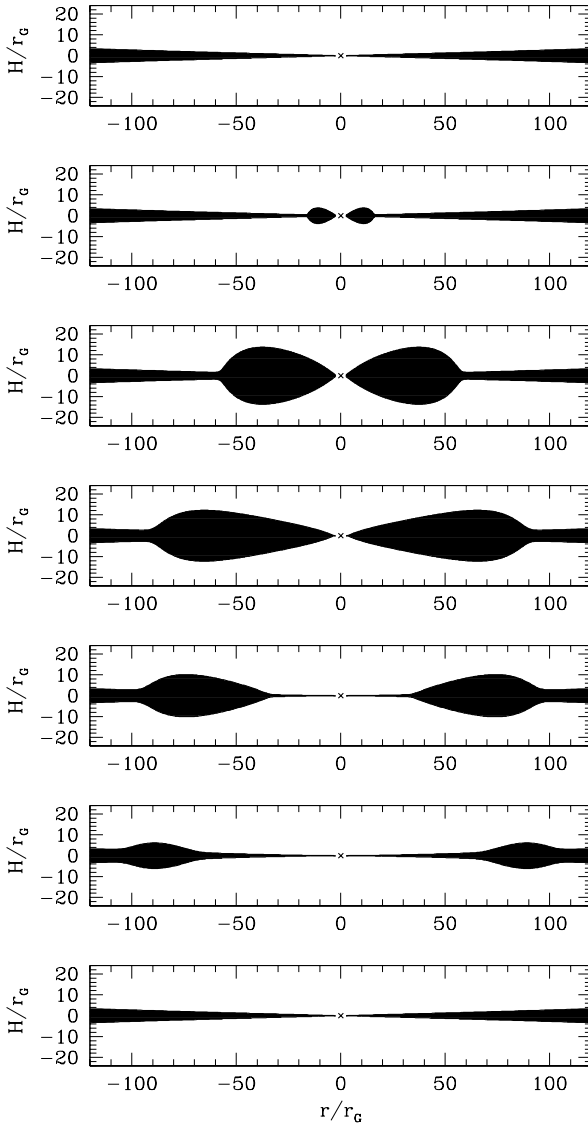


**Figure 1.** The evolution of the geometrical profile of the disc during one full cycle. The sequence of panels shows the situation after 0, 2, 8, 16, 18, 22 and 787 s respectively, starting from the beginning of the cycle. (Note that the outer boundary of the grid is at  $r = 10^4 r_G$ , far beyond the outer edge of the frame shown here.)

cycle, corresponding to the second panel in Fig. 1. At the start of the cycle, the effective optical depth  $\tau_{eff}$  is greater than 100 everywhere but it becomes smaller in the inner parts of the disc as the material there expands, falling below 10 for  $r < 9 r_G$  by the present stage. The behaviour of this and the other quantities is shown by the corresponding curves (marked with dots) in Figs. 2 – 5. (Note that despite their sharp appearance, all of these curves are, in fact, perfectly continuous and well-resolved on the grid as can be seen if they are viewed with a larger spatial resolution.) As the outgoing wave progresses further, the temperature peak is progressively reduced in magnitude although it remains at a level well above that of the initial model. The outgoing wave is heating the material through which it passes, causing the part of the disc internal to it to swell up further as shown

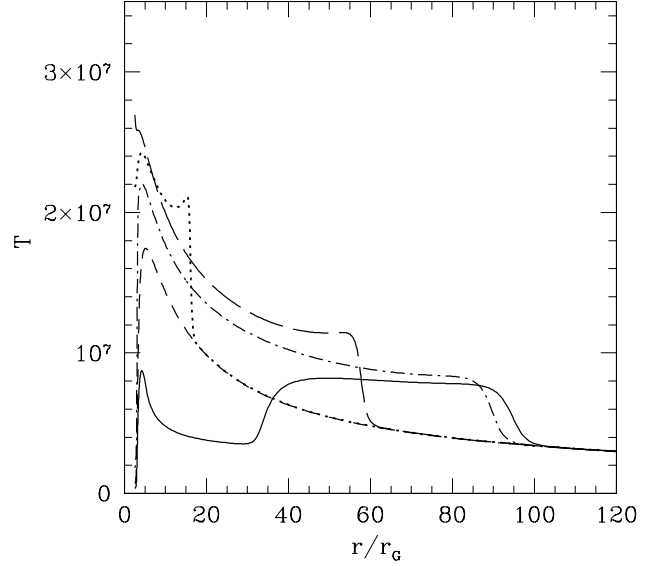


**Figure 2.** The temperature  $T$ , measured in degrees kelvin, is plotted against  $r/r_G$  at successive times during one full cycle. The short-dashed curve shows the temperature at the beginning of the cycle ( $t = 0$  s), the dotted curve is for  $t = 2$  s, the dashed curve is for  $t = 8$  s, the dot-dashed curve is for  $t = 16$  s and the solid curve is for  $t = 18$  s.

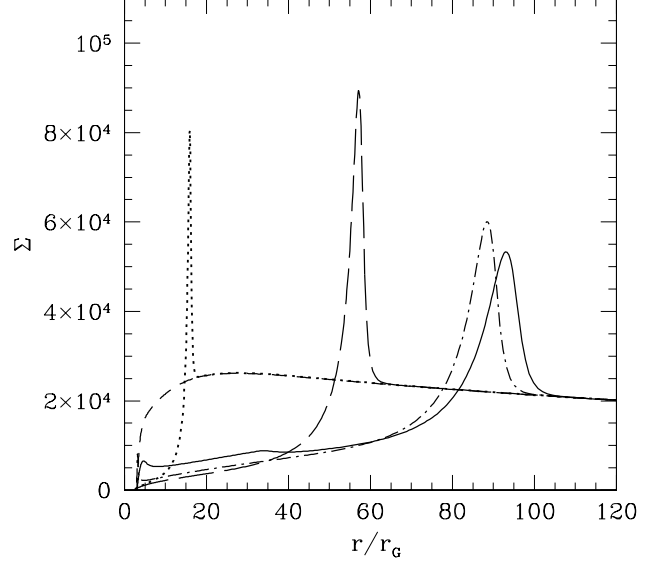


**Figure 3.** The surface density  $\Sigma$ , measured in units of  $\text{g cm}^{-3}$ , is plotted against  $r/r_G$  at the same times as shown in Fig. 2.

in the third panel of Fig. 1. The region with very low effective optical depth ( $\tau_{eff} < 10$ ) is now extending out to  $15 r_G$ . The compression wave is pushing material strongly outwards away from the black hole (note, in Fig. 5, the large negative  $\dot{m}$  associated with it) while, behind it, matter is falling inwards at a rate which is far above that in the stationary state ( $\dot{m} = 0.06$ ) and is even well above the critical accretion rate  $\dot{m} = 1$ . In this initial phase of the evolution, the propagating compression front divides the disc into two parts. The

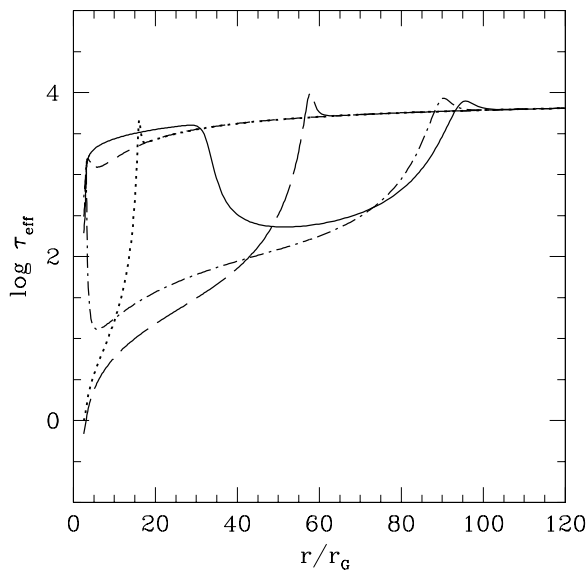


**Figure 4.** The effective optical depth  $\tau_{\text{eff}}$  is plotted against  $r/r_G$  at the same times as shown in Fig. 2.

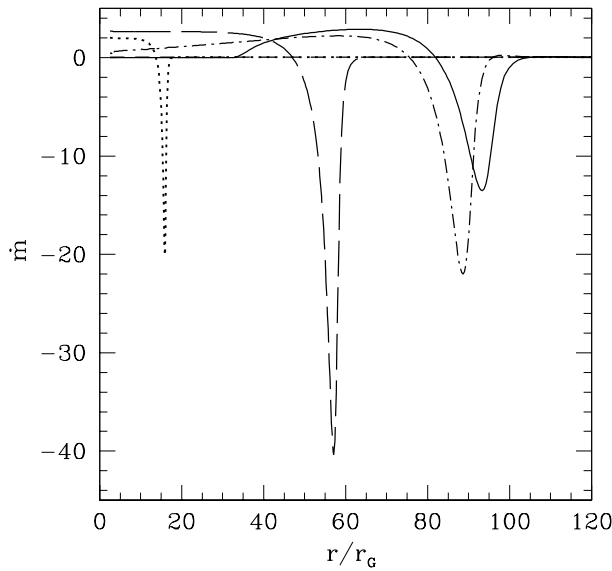


**Figure 5.** The local accretion rate  $\dot{m}(r)$ , measured in units of the critical accretion rate  $\dot{M}_{\text{cr}}$ , is plotted against  $r/r_G$  at the same times as shown in Fig. 2. Negative values of  $\dot{m}$  signify an outflow, ( $\dot{m} = -2\pi r \Sigma v_r$ ).

inner part has a toroidal structure and is characterised by high temperature, low density,  $\tau_{\text{eff}} < 100$ , and a nearly-constant supercritical accretion rate, while the outer part is basically similar to the original unperturbed stationary disc (although, as we will see later, it is actually far from being a stationary flow for cycles after the first one). The width of the transition zone between these two parts increases as the front moves outwards and has reached  $20 r_G$  by 8 seconds into the cycle, corresponding to the third panel of Fig. 1.

In order for the outgoing wave to continue its propagation, it is necessary that the material behind it should

remain in a hot state. Once the wavefront has moved beyond the linearly-unstable region, it becomes progressively harder for the temperature to be maintained in the high state and eventually the front starts to weaken, the temperature drops in the innermost part of the disc and the material there deflates, collapsing down into the equatorial plane. Panel 4 of Fig. 1 shows the situation at the moment when this happens, 16 s into the cycle, and in the subsequent panels 5 and 6 one can see the deflation spreading out through the disc. During the initial collapse, the volume density  $\rho$  rises dramatically at the place where the collapse occurs, growing by a factor of  $10^3$  in less than a second and forming a sharp spike which oscillates and then starts to broaden progressively. (This is a feature which is easy to follow in animations of the data but is hard to show clearly with a static graph.) At the time of panel 4, the accretion rate is decreasing towards the black hole and the optical depth has increased considerably in the inner parts of the disc.

Following this rapid change, the temperature continues to decrease and drops to a low state well below that of the initial model. By the time corresponding to panel 5 of Fig. 1 (18 s after the beginning of the cycle), the compression front is seriously weakening and a growing region of the inner part of the disc has deflated. As can be seen from Fig. 3, there is very little matter inward of the compression front at this stage but the process of refilling the inner part of the disc is now beginning, as the accretion flow near to the black hole is almost turned off. The disc now consists of three different parts. The innermost part forms a geometrically thin disc-like configuration with the temperature and surface density being lower than those of the initial model and with a very low accretion rate. The size of this part is progressively increasing; at 18 s it extends out to just beyond  $30 r_G$ . The middle part is what remains of the toroidal structure. This is still at a higher temperature than in the initial model, is under-dense, has a lowered optical depth and has a high inward accretion rate. The outermost part is still in a similar state to that of the initial model but has been compressed somewhat by the still outward-moving compression front.

At the time of frame 6 of Fig. 1 (22 s after the beginning of the cycle), the first section of the disc (geometrically thin and under-dense) extends out to  $65 r_G$ , the compression front has almost died and the remaining toroidal structure is shrinking away.

This is the end of the “outburst” part of the cycle (which has proceeded on the thermal timescale). What happens next is a slow and uneventful refilling (and reheating) of the inner part of the disc which occurs on the much longer viscous timescale. Finally (787 s after the beginning of the cycle – Fig. 1, 7th panel) the disc has returned to essentially the same state as it was in at the beginning of the cycle. The thermal instability then appears again and a new cycle is initiated.

We have calculated the time evolution of the model up to the beginning of the twenty-first cycle. The cycle period ( $\sim 787$  s) is slightly longer than the 780 s found in our previous study, and it was seen to be gradually increasing with time (albeit with extremely small fractional changes) until a fully relaxed solution was finally obtained. In connection with this, it is important to stress that after the initial time, at which data for a stationary solution was specified, the configuration never again passed through a stationary state

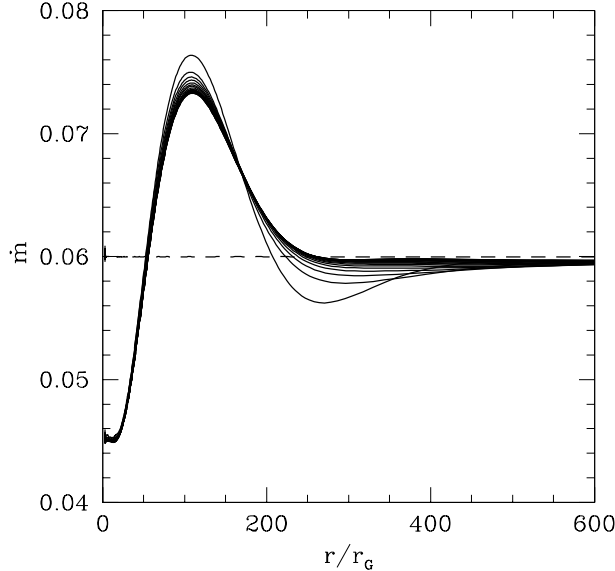


**Figure 6.** The local accretion rate profile at the beginning of successive cycles (note that the vertical scale is very different from that of Fig. 5). The convergence process is rather slow; the final converged profile shows  $\dot{m}$  varying significantly with  $r$  and so represents a genuinely non-stationary solution.

and was not even close to doing so. Figure 6 shows the profile of  $\dot{m}$  at the beginning of successive cycles (just before the instability starts) with the initial model being shown with the dashed line and the subsequent curves being in order of progressively decreasing amplitude. Note that for the fully relaxed case,  $\dot{m}$  has a minimum of 0.045 (near to the black hole) and a maximum of 0.073 (just outside  $100 r_G$ ) and so is far from being constant at 0.06 as was the case for the initial model. In view of this, it is clear that a number of cycles would be needed before a relaxed solution could be obtained and this is the main reason for the progressive change seen in these  $\dot{m}$  curves although there is also some evidence of smoothing related to the parabolic prescription for the viscosity.

Integrating the radiated flux per unit area over the disc at successive times, we have obtained the bolometric light curve shown in Figure 7. The disc luminosity exhibits a burst-like time variation with a burst duration of about 20 s and a quiescent phase lasting for the remaining 767 s of the cycle. The amplitude of the variation is around two orders of magnitude: at the maximum, the luminosity is approximately 40 times larger than it was immediately before the outburst and after the peak it then drops below the pre-burst value by a factor of about 4.5. During the following quiescent phase, it then gradually increases again until the onset of the next outburst.

The bolometric luminosity is not a directly observed quantity, and so even if we expect that most of the energy in galactic black hole candidates will be radiated in the X-ray band, it is necessary to calculate the spectrum emitted from the disc and the light curves in the particular wavebands, in order to perform any detailed comparison with observations. This will be discussed in subsequent papers.

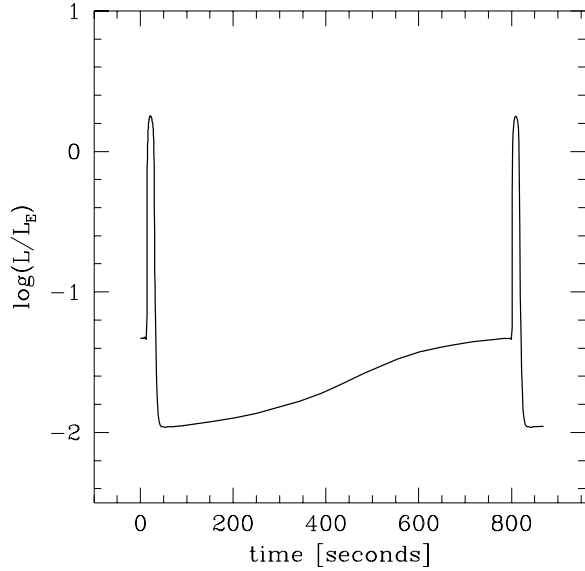


**Figure 7.** Variation of the bolometric luminosity of the disc expressed in units of the Eddington luminosity.

## 5 DISCUSSION AND CONCLUSIONS

In the previous calculations presented in Papers I and II, which we use here for comparison with the results of the present more elaborate study, we investigated the simple slim-disc model with all of its associated assumptions and approximations. Two different values of the viscosity parameter  $\alpha$  (low - 0.001 and high - 0.1) were considered there. In the present work, two important new aspects have been introduced: the diffusion-type formulation for the viscosity and the dynamical treatment of motion in the vertical direction. We now examine some features discussed before for the previous formulation to see how these are changed with the new one.

In Paper I we observed that the supposedly stable model with  $\alpha = 0.001$  and  $L = 0.01 L_E$  did not remain unchanging but instead developed an instability in the region  $3 - 6 r_G$  after  $10 - 20$  s of the evolution (see Figure 11 in Paper I). This appeared first at around  $4.7 - 4.8 r_G$  and then grew rapidly, causing termination of the calculation. The high- $\alpha$  model of Paper II was subject to the same kind of problem. We found that the instability could be suppressed by adding a low level of numerical diffusion to the radial equation of motion and this suggested that additional physical diffusive terms, which were not included in the simple version of the model, might play a key role in avoiding this type of instability. Following our strategy, we repeated the calculation for the thermally-stable model studied in Paper I, using the new version of the code and leaving out the numerical diffusion term. We found that the oscillations do appear again (see Figure 8) but this time they remain bounded at a low level and do not cause termination of the evolution. In particular, we note that they are not trapped around their point of origin but are able to propagate freely outwards. In the case of the high- $\alpha$  model studied here, these oscillations interfere with the developing thermal instability which is, of

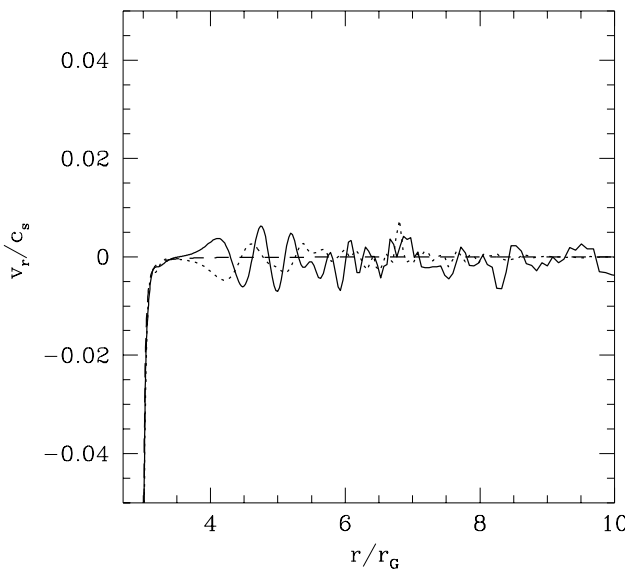


**Figure 8.** Numerical noise which appears when the artificial diffusion term is removed. These velocity curves are for the model with  $\alpha = 0.001$  and  $\dot{m} = 0.01$  at three different times:  $t = 0$  s (dashed line),  $t = 76$  s (dotted line) and  $t = 1881$  s (solid line). Note that the vertical scale is very much expanded with respect to Fig. 11 of Paper I so that the oscillations can be seen.

course, undesirable and so having studied their behaviour under these new circumstances, we then re-introduced the low level of artificial diffusion as before in order to suppress them.

Next we consider the violently unstable feature seen in the calculations presented in Paper I for models with low viscosity and luminosities between  $0.09 L_E$  and  $1 L_E$ . This instability manifested itself as a dramatic shock-like feature which appeared near to the sonic point and then grew rapidly, destroying the calculation. Similar behaviour was seen in equivalent calculations made by Ryoji Matsumoto (private communication) using a different numerical method. The nature of this behaviour is still under study. If not avoided or saturated, it would lead to disruption of the disc meaning that models like these would not be suitable for describing persistent astronomical flow configurations. We made a detailed investigation of the effect of introducing different forms of artificial viscosity or diffusion and found that none of these could act to limit the instability unless they were increased to levels which did not seem reasonable. We emphasise that our numerical code has no difficulty in dealing with ordinary shock structures and, indeed, in Paper II we showed a disc evolution with strong shocks present in the supersonic part of the flow. In fact, despite first impressions, the dynamically growing feature turns out not actually to be a shock but, instead, is a transient feature across which the Rankine-Hugoniot conditions are not satisfied. It is therefore not particularly surprising that methods designed for handling shocks were not successful in dealing with this. By adding a large enough amount of viscous dissipation, the disruptive nature of the feature can indeed be removed but our feeling was that introducing so much diffusion without physical motivation was unwarranted (as we said in Section 4 of Paper II). At that stage, we wanted

to wait for the introduction of a  $(\partial\Omega/\partial r)$  viscosity to see the effect of that before proceeding further. Perhaps a good description of the feature is that it is like a wave washing up against a sea-wall with the density gradient near to the sonic point playing the role of the wall. When sufficiently high artificial diffusion was added, the wave was seen to fall back from the wall and then to wash up against it again repeatedly but without disrupting the rest of the solution. The introduction of the additional features in our current code has not turned out to be sufficient, in itself, to avoid the instability destroying the solution unless similarly high levels of artificial diffusion continue to be added.

Our original plan was to perform a systematic study of disc evolution with additional effects being added one at a time but here we have gone against this by introducing, at the same time, the diffusive  $(\partial\Omega/\partial r)$  viscosity prescription and the dynamical treatment of motion in the vertical direction. The reason for this was because of a computational difficulty which we encountered with the new viscosity prescription at the stage when the vertically-expanded part of the disc started to deflate. All of our attempts to calculate through this stage with the  $\partial\Omega/\partial r$  viscosity were unsuccessful until we decided to introduce also the vertical acceleration, at which point the problem disappeared. It seems that the approximate nature of the  $\alpha p$  prescription somehow compensated the similarly doubtful use of the condition of vertical hydrostatic equilibrium.

In our calculations, we have reported two main types of time-varying behaviour for models undergoing the thermal instability: for our higher value of  $\alpha$  ( $= 0.1$ ), we have seen limit-cycles, while for low  $\alpha$  ( $= 0.001$ ), we saw a seemingly catastrophic instability. Takeuchi & Mineshige (1998) have presented extremely interesting results from an  $\alpha p$  calculation for very high  $\alpha$  ( $= 1$ ) in which they see an evolution which starts in the same way as our model which makes limit cycles but, after the general deflation, a small inflated, optically thin region remains at the inner edge of the disc (inward of  $r = 5 r_g$ ) which seems to be a persistent ADAF-like feature. This blocks the possibility of starting a new outburst cycle. The authors give a persuasive argument for why this should occur, indicating that there should be a difference in behaviour for models with  $\alpha > 0.3$ , for which the expanded states are fully optically thin (our model with  $\alpha = 0.1$  has considerably reduced optical depth in the expanded region but only has  $\tau_{eff} < 1$  briefly and then only for a very small region at the inner edge of the disc). When we have, in the past, tried to make calculations for  $\alpha = 1$ , we experienced difficulty in keeping the code numerically stable (and there is, perhaps, evidence of some similar problem in the graphs shown by Takeuchi & Mineshige, although we stress that we find their results believable, particularly in view of the supporting arguments which they present). Clearly, it is now of interest for us to return to those calculations and see whether we can confirm the results of Takeuchi & Mineshige. In particular, it will be interesting to see whether the persistent ADAF feature would survive changing the viscosity prescription to the diffusive form.

In conclusion: the main result of our present paper concerns the effect of replacing the  $\alpha p$  viscosity prescription by the more physical diffusive form when calculating the global evolution of the thermal instability, driven by radiation pressure, for a vertically-integrated model of a non-

self-gravitating transonic accretion disc in the high- $\alpha$  case ( $\alpha = 0.1$ ). We find that the evolution remains cyclic in character and is very little changed from that seen before. This provides some strengthened motivation for saying that the type of disc behaviour seen in our calculations might truly have some fundamental importance. It is then natural to proceed with studying the possibility that its effects might be present among the range of different variability patterns observed for accreting compact objects. The transonic discs described here with accretion rates larger than a certain value (which depends on the mass of the central black hole,  $M$ , and the viscosity parameter,  $\alpha$ ) are not stationary but show a cyclic behaviour which can be characterised by the period of the cycles, the durations of the bursting phase and of the quiescence, and the amplitude and shape of the burst. For different input parameters:  $M$ ,  $\alpha$ ,  $\dot{m}$ , we should expect to see different characteristics. A straightforward comparison with XTE observations, for example, can lead to identification of sources where the thermal limit-cycle behaviour may be responsible for observed variabilities. So far, there is only one source for which this mechanism has been proposed: GRS 1915+105 (Belloni et al. 1997) and the situation for that is still under investigation. Good quality data are now available for making a detailed confrontation with clear model predictions.

## ACKNOWLEDGMENTS

We gratefully acknowledge financial support from the Polish State Committee for Scientific Research (grant KBN 2P03D01817), the Italian Ministero dell'Università e della Ricerca Scientifica e Tecnologica, the Italian INFN and the European Union (under the EU programme ‘‘Improving the Human Research Potential and the Socio-Economic Knowledge Base’’: RTN contract HPRN-CT-2000-00137).

## REFERENCES

Abramowicz M.A., Czerny B., Lasota J.-P., Szuszkiewicz E., 1988, *ApJ*, 332, 646  
 Artemova I.V., Bisnovatyi-Kogan G.S., Igumenshchev I.V., Novikov I.D., 2001, *ApJ*, 549, 1050  
 Balbus S.A., Hawley J.F., 1991, *ApJ*, 376, 214  
 Balbus S.A., Papaloizou, J.C.B., 1999, *ApJ*, 521, 650  
 Belloni T., Méndez M., King A.R., van der Klis M., van Paradijs J., 1997, *ApJ*, 479, L145  
 Chen X., Taam R.E., 1993, *ApJ*, 412, 254  
 Hawley J.F., Balbus S.A., Stone J.M., 2001, *ApJL*, 554, 49  
 Honma F., Matsumoto R., Kato S., 1991, *PASJ*, 43, 147  
 Hoshi R., Shibasaki N., 1977, *Prog. Theor. Phys.*, 58, 1759  
 Kato S., Fukue J., Mineshige S., 1998, *Black Hole Accretion Disks* (Kyoto: Kyoto University Press)  
 Papaloizou J.C.B., Szuszkiewicz E., 1994a, in Proc. 33rd Herstmonceux Conf., *The Nature of Compact Objects in Active Galactic Nuclei*, A. Robinson & R. Terlevich, eds., Cambridge University Press, Cambridge  
 Papaloizou J.C.B., Szuszkiewicz E., 1994b, *MNRAS*, 268, 29  
 Shakura N.I., Sunyaev R.A., 1973, *A&A*, 24, 337  
 Shibasaki N., 1978, *Prog. Theor. Phys.*, 60, 985  
 Szuszkiewicz E., Miller J.C., 1997, *MNRAS*, 287, 165  
 Szuszkiewicz E., Miller J.C., 1998, *MNRAS*, 298, 888  
 Takeuchi M., Mineshige S., 1998, *ApJ*, 505, L19  
 von Weizsäcker C.F., 1948, *Z. Naturforsch.* 3a, 524

This paper has been produced using the Royal Astronomical Society/Blackwell Science TeX macros.